

Amino acid supplementation confers protection to red blood cells prior to Plasmodium falciparum bystander stress

Tracking no: ADV-2023-010820R2

Heather Binns (Wake Forest University, United States) Elmira Alipour (Wake Forest University, United States) Cameron Sherlock (Wake Forest University, United States) Dinah Nahid (Wake Forest University, United States) John Whitesides (Wake Forest University School of Medicine, United States) Anderson Cox (Wake Forest University School of Medicine, United States) Cristina Furdul (Wake Forest University School of Medicine, United States) Glen Marrs (Wake Forest University, United States) Daniel Kim-Shapiro (Wake Forest University, United States) Regina Cordy (Wake Forest University, United States)

Abstract:

Malaria is a highly oxidative parasitic disease in which anemia is the most common clinical symptom. A major contributor to malarial anemia pathogenesis is the destruction of bystander, uninfected red blood cells (RBCs). Metabolic fluctuations are known to occur in the plasma of individuals with acute malaria, emphasizing the role of metabolic changes in disease progression and severity. Here, we report that conditioned media from Plasmodium falciparum culture induces oxidative stress in uninfected, catalase-depleted RBCs. As cell permeable precursors to glutathione, we show a benefit of pre-exposure to exogenous glutamine, cysteine, and glycine (QCG) amino acids for RBCs and that this pre-treatment intrinsically prepares RBCs to mitigate oxidative stress.

Conflict of interest: No COI declared

COI notes:

Preprint server: Yes; BioRxiv 10.1101/2023.05.16.540951

Author contributions and disclosures: R.J.C. and H.C.B. designed and conceptualized the project; H.C.B. performed and analyzed the results of the experiments, designed the figures, and wrote the initial manuscript. C.E.B. performed a subset of experiments. E.A. performed and analyzed ektacytometry experiments. D.S.N. performed parasite culture and conditioned media generation. J.F.W. contributed technical expertise for flow cytometry experiments. A.O.C. performed mass spectrometry experiments. C.M.F. supervised mass spectrometry and contributed redox biology expertise. G.S.M. assisted with microscopy experiments and contributed technical expertise for fluorescent and scanning electron microscopy imaging. D.B.K-S. supervised ektacytometry, contributed red cell biophysics expertise, and contributed to the overall experimental design. R.J.C. supervised the experiments, data analysis, and revising of the manuscript. All authors contributed to and endorsed the final version of the manuscript.

Non-author contributions and disclosures: No;

Agreement to Share Publication-Related Data and Data Sharing Statement: emails to the corresponding author

Clinical trial registration information (if any):

1

2 **Amino acid supplementation confers protection to red blood cells prior to**
3 ***Plasmodium falciparum* bystander stress**

4

5

6 Heather Colvin Binns^{1,2}, Elmira Alipour³, Cameron E. Sherlock¹, Dinah S. Nahid¹, John
7 F. Whitesides², Anderson O'Brien Cox⁴, Cristina M. Furdui^{4,5}, Glen S. Marrs¹, Daniel B.
8 Kim-Shapiro³, Regina Joice Cordy^{1,2}

9

10

11 ¹Department of Biology, Wake Forest University, Winston-Salem, North Carolina, USA

12 ²Department of Microbiology and Immunology, Wake Forest University School of
13 Medicine, Winston-Salem, North Carolina, USA

14 ³Department of Physics, Wake Forest University, Winston-Salem, North Carolina, USA

15 ⁴Proteomics and Metabolomics Shared Resource, Comprehensive Cancer Center, Wake
16 Forest University School of Medicine, Winston-Salem, North Carolina.

17 ⁵Department of Internal Medicine, Section on Molecular Medicine, Wake Forest
18 University School of Medicine, Winston-Salem, North Carolina, USA

19

20 **Corresponding Author**

21 Wake Forest University

22 Biology

23 1834 Wake Forest Rd

24 Winston Hall Room 211

25 Winston Salem, North Carolina 27109

26 United States

27 cordyrj@wfu.edu

28

29 **Data Sharing**

30 emails to the corresponding author

31

32 **Abstract**

33 Malaria is a highly oxidative parasitic disease in which anemia is the most common
34 clinical symptom. A major contributor to malarial anemia pathogenesis is the destruction
35 of bystander, uninfected red blood cells (RBCs). Metabolic fluctuations are known to
36 occur in the plasma of individuals with acute malaria, emphasizing the role of metabolic
37 changes in disease progression and severity. Here, we report that conditioned media
38 from *Plasmodium falciparum* culture induces oxidative stress in uninfected, catalase-
39 depleted RBCs. As cell permeable precursors to glutathione, we show a benefit of pre-
40 exposure to exogenous glutamine, cysteine, and glycine (QCG) amino acids for RBCs
41 and that this pre-treatment intrinsically prepares RBCs to mitigate oxidative stress.

42

43

44 **Key points**

- 45 • Intracellular reactive oxygen species (ROS) is acquired in red blood cells (RBCs)
46 incubated with *Plasmodium falciparum* conditioned media
- 47 • Glutamine, cysteine, and glycine amino acid supplementation led to increased
48 glutathione biosynthesis and reduced ROS levels within stressed RBCs

49

50

51 **Introduction**

52 Anemia is the most common clinical consequence of human malaria, a parasitic disease
53 with nearly 250 million cases annually¹. Pathogenesis of malarial anemia is multifaceted
54 consisting of a loss of both infected and uninfected red blood cells (RBCs) as well as
55 dysregulation of new RBC production². In malaria infections caused by *P. falciparum*,
56 uninfected RBCs are lost at a much greater rate than infected RBCs. This so called
57 “bystander effect” occurs prior to adaptive immune system activation³, contributing

58 greatly to the development of malarial anemia. The mechanisms of the malarial
59 bystander effect on uninfected RBCs are unclear, although a loss in membrane
60 deformability is known to contribute to the removal of bystander RBCs from circulation^{4,5}.
61 Bystander RBCs have also been shown to undergo cell surface changes promoting
62 erythrophagocytosis through both complement-mediated activation⁶ and
63 phosphatidylserine antibody-mediated removal⁷. *In vivo* models for malaria demonstrate
64 that over 75% of the RBCs that are lost are uninfected during naïve infection, while only
65 ~5% of all RBCs destroyed during infection are due to direct parasite infection with
66 inhibition of erythropoiesis making up the remaining portion⁸. Culture medium from *P.*
67 *falciparum*-infected RBCs was shown to impact biological function of nucleated erythroid
68 cells⁹. In addition, parasite-derived mitochondrial DNA within the media of *P. falciparum*
69 parasite culture was found to elicit toll-like receptor 9 (TLR9) binding, thereby altering the
70 membranes of healthy RBCs¹⁰. Interrupted glycolysis also increases RBC susceptibility
71 to senescence and oxidative damage and further highlights the importance of the
72 exogenous metabolic environment for RBCs¹¹. These previous findings indicate multiple
73 mechanisms contributing to the bystander effect in malaria.

74

75 While mature RBCs have limited metabolic activity due to a lack of membrane-bound
76 organelles, these cells have multiple active antioxidant components to counter oxidative
77 stress in their environment. These intracellular defenses include reduced glutathione
78 (GSH), catalase, peroxiredoxins, and glutathione peroxidase^{12,13}. Oxidative stress plays
79 a major role in many anemia-inducing conditions, such as malaria and sickle cell disease
80 (SCD)^{14,15}. In malaria, RBCs from patients have reduced levels of intracellular catalase¹⁶,
81 indicating these cells are deficient in their ability of fully combatting oxidative stress and
82 rendering avenues of antioxidant therapy as a viable treatment to lessen disease
83 severity. Exogenous GSH, a potent antioxidant, is structurally unable to freely permeate

84 cellular membranes; therefore, individual amino acid building blocks of the tripeptide
85 GSH (glutamine, cysteine, and glycine) are taken up by RBCs which perform *de novo*
86 GSH biosynthesis inside the cell¹⁷. Additionally, significant host metabolic alterations
87 occur during malaria. This includes markedly reduced levels of plasma free amino acids
88 such as glutamine and arginine^{18–25}, suggesting amino acid supplementation could
89 perhaps provide therapeutic benefit in malaria.

90
91 Oral treatment with L-glutamine (Gln) is a recently approved therapy for sickle cell
92 disease²⁶. While the exact cellular mechanism remains unclear, a potential role for Gln is
93 to improve the nicotinamide adenine dinucleotide phosphate (NADPH) stores in sickled
94 RBCs²⁷, lessening the oxidative stress. Gln also serves as a precursor for arginine, an
95 amino acid that has been inversely associated with mortality in cerebral malaria²² and
96 proposed to be beneficial in both malaria²⁸ and sickle cell disease²⁹. Gln is also
97 implicated in malarial anemia where low plasma Gln levels were found to be associated
98 with severe pediatric malarial anemia³⁰. Here, we explore the oxidative impact of the *P.*
99 *falciparum* culture environment on uninfected, catalase-inhibited RBCs as a proxy for *in*
100 *vivo* severe malaria bystander effect. Furthermore, we investigate the role of exogenous
101 amino acid supplementation on bystander RBCs and show that RBCs pretreated with
102 precursor antioxidant amino acids glutamine, cysteine, and glycine concomitantly have
103 increased intracellular glutathione synthesis and thus these amino acids together confer
104 protection from oxidative stress.

105

106

107 **Methods**

108 *Blood washing and perturbations*

109 Heparinized venous blood, Type O+, was collected from healthy adult participants with
110 informed consent and used with approval from Wake Forest University Institutional
111 Review Board (Study ID: IRB00024199) or was commercially purchased from BioIVT Inc
112 and received within 24 hours of collection. Briefly, RBCs were washed three times in
113 excess 1X Phosphate Buffered Saline (PBS), pH 7.4 (Gibco™ □) and centrifuged at 900
114 x g to remove plasma and buffy coat layers with each wash. Washed RBCs were stored
115 in 1X PBS supplemented with 5 mM D-glucose (PBS+Gluc) and used the same day. All
116 RBC incubation experiments were performed at 1% hematocrit (hct) while rocking at
117 37°C. Overnight 24-hour incubations were performed for amino acid supplementation
118 and *P. falciparum* conditioned medium (*PfCM*) stress. For amino acid supplementation
119 experiments, indicated concentrations of amino acids were thoroughly dissolved in
120 PBS+Gluc and incubated overnight. The amino acid concentrations were selected to be
121 1000 μM to approximate the average glutamine concentration in plasma of patients with
122 SCD treated with L-glutamine²⁷ which is also in the realm of levels of glutamine in
123 Kenyan children with malaria but without SMA (mean of 1361 μM for those without SMA
124 as compared to 484 μM for those with SMA).³⁰ Cells were then washed twice in PBS to
125 remove amino acids prior to stress incubations. All hydrogen peroxide perturbations
126 were performed in the presence of 1 mM sodium azide (NaN₃) to block intracellular
127 catalase activity and incubated for 15-minutes while rocking at 37°C, as described
128 previously^{31–33}. *PfCM* perturbations were also performed with 1 mM NaN₃ to block
129 intracellular catalase activity. Control media conditions for *PfCM* perturbations included
130 RPMI 1640 (Gibco™ □) supplemented with 1 mM NaN₃.

131

132 *Plasmodium falciparum* culture and conditioned media

133 *Plasmodium falciparum* of the 3D7 laboratory strain (MRA-102; BEI Resources) was
134 used in the generation of *PfCM*. RBCs were combined from two O+ donors at 2% hct
135 and maintained in standard culture media consisting of RPMI 1640 (Gibco™ □)
136 supplemented with sodium bicarbonate, HEPES buffer, hypoxanthine, gentamicin, and
137 0.5% (wt/vol) Albumax II³⁴ in a gas environment of 1% O₂, 5% CO₂, and 94% N₂.
138 Parasites were synchronized using a 5% Sorbitol solution, seeded at 0.4% parasitemia,
139 and allowed to grow with no media change, but one gas exchange, for 72 hours. The
140 culture was then centrifuged at 600 x g for 15 minutes, then 1600 x g, then 3600 x g, and
141 then filtered with a 0.45 μm filter, before storing at 4°C, as described previously³⁵. For
142 glucose supplementation experiments, 5.5 mM D-glucose was dissolved into *PfCM* and
143 RPMI 1640 base media, respectively. The value of 5.5 mM was selected as being on the
144 high end of the human fasting glucose range (3.9.- 5.6 mM) and approximately 50% of
145 the concentration of D-glucose in fresh RPMI (11.1 mM).

146

147 *Intracellular ROS detection*

148 Intracellular ROS was measured using a Cellular ROS Assay Kit (ab113851; Abcam).
149 Washed RBCs were incubated with a 2 μM working concentration of 2',7' –
150 dichlorofluorescein diacetate (DCFDA) for 30 minutes. RBCs were then washed twice
151 with 1X PBS and used for either flow cytometry analysis or live cell imaging.

152

153 *Flow cytometry*

154 RBCs were analyzed by either a BD LSRFortessa™ □ X-20 Flow Cytometer (Becton
155 Dickinson) or a CytoFLEX V0-B3-R1 Flow Cytometer (Beckman Coulter). RBCs were
156 passed at a flow rate of about 5,000 cells per second. Samples ran on the BD
157 LSRFortessa™ X-20 Flow Cytometer (Becton Dickinson) utilized a 60 milliwatt 488 nm
158 laser at 550 volts for excitation and a green (505 longpass and 530/30 bandpass),

159 fluorescein isothiocyanate (FITC) emission filter for detection. Samples ran on the
160 CytoFLEX V0-B3-R1 Flow Cytometer (Beckman Coulter) utilized a 50 milliwatt 488 nm
161 laser for excitation and a 525/40 band pass emission filter for detection. For data
162 analysis, mean fluorescent intensity was measured for 100,000 events, gated on doublet
163 discrimination (FSC-H vs FSC-A), and analyzed using FCS Express 7 Research
164 software (De Novo).

165

166 *Live cell imaging*

167 Experiments were carried out using a Leica Thunder Live Cell Imaging System and LasX
168 acquisition software. Images were acquired as 16-bit data with a Leica K8 sCMOS
169 camera (2048 X 2048 pixels), using a 63X Plan Apo oil immersion lens (1.4NA). RBCs
170 were plated onto 35 mm optical coverglass dishes (Ibidi) immediately before imaging.
171 For time lapse experiments, images were acquired every 15 seconds. All
172 excitation/acquisition parameters were held constant across imaging experiments
173 including light-emitting diode excitation level and camera exposure time. All analyses
174 were performed using Leica instantaneous computation clearing intensity (ICC) values.
175 For analysis, stationary cells were chosen using Differential Interference Contrast
176 images and isolated using region of interest selection using FIJI³⁶. Fluorescence in
177 regions of interest was quantified from ICC adjusted images at each timeframe image.
178 Data was normalized to average fluorescence of first three timepoints, prior to treatment.
179 For visualization purposes, images were adjusted to maximize for brightness contrast
180 using FIJI³⁶.

181

182 *Scanning electron microscopy*

183 Perturbed RBCs were washed and fixed in an osmotic-controlled glutaraldehyde
184 solution, as previously reported . Briefly, glutaraldehyde-fixed RBCs were washed and

185 resuspended in distilled H₂O at 0.5% hct before air drying overnight on 12mm round
186 coverslips at 60°C. Images were collected with Everhart-Thornley secondary electron
187 detection using either an AMRAY 1810 or a Phenom XL scanning electron microscope
188 at 10Kv accelerating voltage. Typical magnifications employed were 2000X to allow for
189 high resolution of RBCs while maintaining a reasonable field size. Samples were
190 prepared for imaging by first dehydrating on carbon tab aluminum stubs, then gold
191 sputter coating under argon gas conditions to a thickness of about 7-10nm. Echinocyte
192 morphology stages were defined as previously described³⁸⁻⁴⁰ and total number of cells in
193 two fields of view were imaged and quantified for morphology scoring. Each field of view
194 had varying total cells on slide (range: 131-384 cells) and so the morphology scores and
195 stages were reported per 100 cells to account for this variation per independently
196 imaged field of view.

197

198 *Osmotic gradient ektacytometry*

199 A Technicon osmotic gradient ektacytometer (Technicon Instrument Corp.) facilitated the
200 deformability measurements of the RBCs. Thirty-one (31) g/L of polyvinylpyrrolidone
201 (PVP) polymer (Sigma, 437190) mixed with 0.9 g/L of sodium phosphate dibasic
202 anhydrous Na₂HPO₄ (Fisher, 7558-79-4), 0.24 g/L of sodium phosphate monobasic
203 NaH₂PO₄ (Fisher Biotech, 10049-21-5), and 0.544 g/L of sodium chloride NaCl (Sigma,
204 S7653) was prepared in Milli-Q ultrapure water with the pH of 7.4. The “low” solution (40
205 mOsm) was used to make the “high” (750 mOsm) and “sample” solutions, by dissolving
206 11.25 g of NaCl in 500 mL of the low solution, and 1.9782 g of NaCl in 250 mL of the low
207 solution (290 mOsm), respectively. After calibration using known osmolality mixtures and
208 finding the required parameters as well as laser alignment of the ektacytometer, 150 µL
209 of the blood samples (40% hematocrit) was diluted into 4 mL of sample solution. The
210 population of RBCs suspended in high viscous media was directed into the gap between

211 two coaxial cylinders. The outer cylinder stayed motionless while the inner cylinder
212 rotated with distinct angular velocity to apply the defined shear stress of 159 dynes/cm^2
213 (~ 16 pascals) at a controlled temperature. During operation, the focused laser beam
214 passed through the suspension and generated elliptical diffraction patterns of the flowing
215 RBCs projected on a detector. LabVIEW software recorded the diffraction patterns and
216 the corresponding osmoscans and quantitative statistics. Data was fit using Origin 2016
217 software and the averages of three separate scans from each blood sample were
218 analyzed. GraphPad Prism was used for the graphing of the recorded result.

219

220 *DNA extraction and amplification*

221 Following PfCM exposure, RBCs were washed in 1X PBS (Gibco) and DNA was
222 extracted from samples using a commercially available kit (K0781; Thermo Fisher
223 Scientific). Quantitative PCR amplification of a 500bp fragment of the *P.falciparum*
224 mitochondrial cytochrome c oxidase subunit III (coxIII) gene using primers previously
225 developed¹⁰ was performed using PowerTrack™ SYBR green Master Mix (A46012;
226 Thermo Fisher Scientific) and a Roche LightCycler 480. Cycle threshold (Ct) and
227 baseline threshold values were calculated using the Roche LightCycler 480 software.

228

229 *Metabolite extraction*

230 Following perturbation experiments, 1×10^7 RBCs were pelleted and the supernatant was
231 carefully removed. Pelleted cells were resuspended in 1X PBS with 100 mM N-
232 ethylmaleimide (NEM) (Cat#128-53-0, Millipore Sigma) for 15 minutes at room
233 temperature³¹. Following NEM incubation, cells were washed twice with 1X PBS. After
234 thorough removal of NEM from supernatant, PBS was added with a final cell
235 concentration of 20% hct and cell concentration was recorded using a hemocytometer.
236 Methanol was added (4:1) followed by vortexing and storing cells on ice for 30 minutes.

237 Sample tubes were then centrifuged at 18,000 x g and supernatant was carefully
238 removed and stored in -80°C for mass spectrometry analysis.
239
240 *Targeted Mass Spectrometry*
241 Targeted LC-MS/MS analysis was performed at the Proteomics and Metabolomics
242 Shared Resource (Wake Forest University School of Medicine, Winston Salem, NC).
243 Briefly, extracted samples were dehydrated and reconstituted in H₂O followed by mass
244 spectrometry (Sciex 7500 MS) analysis⁴¹ for relative quantification of reduced
245 glutathione (GSH alkylated by NEM) and oxidized glutathione (GSSG) metabolites,
246 without any further derivatization⁴². Separation was performed on a Thermo Scientific
247 Hypersil GOLD aQ reverse phase column (2.1 x 150 mm, 3µm) with a gradient mobile
248 phase system consisting of an aqueous phase of 0.1% formic acid (A) and an organic
249 phase of acetonitrile (B) at a flow rate of 0.5 mL/min (0 - 0.5 min, 0.5-5% B; 0.5 - 6.5
250 min, 5-98% B; 6.5 min-9 min, 98% B). The mass spectrometer used the following source
251 parameters: Ion source gas 1: 35 psi, Ion source gas 2: 70 psi, Curtain gas: 40 psi, CAD
252 gas: 9 psi, Source temperature: 250°C, Spray voltage: 5500 V. Transition masses for
253 targeted analysis were 433.00 > 304.00 m/z (NEM-labeled GSH), and 613.20 > 355.25,
254 613.20 > 484.20 and 613.20 > 231.05 m/z for GSSG. Relative peak intensity values
255 were normalized to 10⁶ cells per sample. Total glutathione levels were determined by
256 adding intensities of GSH-NEM and GSSG with correction for ionization efficiency.
257 Heparinized venous blood, Type O+, was collected from healthy adult participants with
258 informed consent and used with approval from Wake Forest University Institutional
259 Review Board (Study ID: IRB00024199) or commercially purchased from BioIVT Inc.
260
261 **Results**

262

263 **Exogenous Gln alone is not sufficient but exogenous amino acid cocktail reduces**
264 **oxidative stress acquired from H₂O₂**

265 Gln's relevance in both malaria and sickle cell anemia along with it being a cell-
266 permeable precursor to GSH, lead us to first to explore the impact exogenous Gln
267 supplementation on oxidative stress in RBCs. For these studies, we used the
268 intracellular fluorescent ROS indicator, DCFDA. To verify that measured changes are
269 indeed due to ROS and not the result of nonspecific effects from the DCFDA probe, we
270 (a) tested and verified that mean fluorescent intensity increases linearly with hydrogen
271 peroxide concentrations (**Supplemental Figure 1**) and (b) tested and verified that cells
272 pretreated with amino acids in the absence of H₂O₂ stress have no observable change in
273 mean fluorescence intensity compared to the cells incubated with PBS + gluc
274 (**Supplemental Figure 2**). Despite a clear significant difference in intracellular ROS
275 levels upon H₂O₂ treatment (fold change of 1.0 for 0 μM H₂O₂ vs 4.1 for 50 μM H₂O₂, p =
276 0.036), we found no difference between H₂O₂-stressed RBCs pre-exposed to control null
277 media or media supplemented with Gln overnight (**Figure 1A**).

278

279 As H₂O₂ is known to impair RBC function through reduced RBC membrane deformability
280 and cellular dehydration^{32,33,43}, we assessed the osmotic effect⁴⁴ of Gln supplementation
281 and saw an expected decrease in membrane deformability, as measured by DI_{max}, in
282 response to H₂O₂ (0.385 DI_{max} for 0 μM H₂O₂ vs 0.360 DI_{max} 50 μM H₂O₂, p = 0.035).
283 However, RBCs supplemented with Gln had a similar loss in deformability when
284 stressed with H₂O₂, suggesting no impact of Gln on that parameter (**Figure 1B and 1C**).

285

286 In terms of cell hydration, we observed slight dehydration in RBCs stressed by H₂O₂ that
287 bordered on significance (347 mOsm/kg for 0 μM H₂O₂ vs 340 mOsm/kg for 50 μM H₂O₂,

288 p = 0.061), but more interestingly, we found that Gln supplementation significantly
289 improved hydration status compared to RBCs not supplemented with Gln (340 mOsm/kg
290 for 0 μ M Gln vs 344 mOsm/kg 1000 μ M Gln, p = 0.031) (**Figure 1D**). These data
291 demonstrate that Gln supplementation prior to oxidative stress is osmotically
292 advantageous for RBCs hydration but does not improve RBC membrane deformability
293 nor reduce intracellular ROS generation in RBCs.

294

295 Although Gln supplementation alone did not seem to protect RBCs from oxidative stress,
296 Gln is a precursor for glutamate which is required, in addition to cysteine and glycine, for
297 *de novo* GSH synthesis inside the RBC to combat high levels of oxidative stress^{45,46}. We
298 incorporated those additional amino acids into our approach and found that RBCs
299 exogenously pretreated with Gln (Q), cysteine (C), and glycine (G) together, hereby
300 referred to as QCG, incurred significantly less intracellular ROS when stressed with
301 H₂O₂ (mean fold change of 5.0 without QCG vs 4.0 with 1000 μ M QCG pre-treatment, p
302 = 0.009) (**Figure 2A**). This oxidative protection was most notably conferred from 1000
303 μ M QCG supplementation. We also found RBCs pre-exposed to QCG had a significant
304 reduction in loss of membrane deformability once stressed with H₂O₂ (**Figures 2B-C**),
305 although the 1000 μ M QCG concentration of pretreatment did not reach significance (p =
306 0.068). Similar to Gln supplementation, QCG pretreatment resulted in significantly higher
307 hydration status in RBCs (340 mOsm/kg without QCG vs 350 mOsm/kg with QCG,
308 p=0.021), as measured by O_{hyp} (**Figures 2B and 2D**). Reduction in oxidative stress in
309 RBCs pre-exposed to QCG was synergistic compared to effects from individual amino
310 acid pre-treatment alone (**Supplemental Figure 2**). As a comparison with QCG, we also
311 tested the impact of arginine amino acid supplementation as it has been reported to be
312 beneficial in both sickle cell anemia and malaria studies; however, exogenous arginine

313 supplementation did not provide a significant intracellular oxidative advantage to RBCs
314 **(Supplemental Figure 2)**,

315

316 ***P. falciparum*-conditioned medium induces stress in human RBCs**

317 To determine the oxidative impact of *P. falciparum* conditioned medium (*PfCM*) on
318 uninfected, catalase-depleted RBCs, we measured RBC echinocytosis, a morphological
319 change associated with oxidative stress⁴⁷. We observed that RBCs exposed to *PfCM*
320 had significantly higher morphology scores (mean score of 116 for control vs. 138 for
321 *PfCM*, $p = 0.0002$) **(Figure 3A)** and a higher percentage of echinocytes (mean of 10.5%
322 for control vs. 24.9% for *PfCM*, $p = 0.002$) **(Figure 3B)**, as compared to RBCs in control
323 RPMI media. Although overall RBC morphology stages showed slight variations
324 between participants, more severe echinocyte stages were present in RBCs from all
325 participants exposed to *PfCM* **(Supplemental Figure 3)**. Next, we aimed to determine
326 whether redox state was affected in mature RBCs alongside the change in morphology.
327 RBCs incubated with *PfCM* had a significant increase in intracellular ROS as detected
328 by DCFDA, compared to RBCs from the same donor exposed to control media (fold
329 change of 1.0 for control vs. 1.8 for *PfCM*, $p = 0.011$) **(Figure 3C-D)**. To confirm the
330 *PfCM*-induced oxidative stress was not due to known depleted levels of glucose during
331 *P. falciparum in vitro* cultivation⁴⁸, we supplemented *PfCM* and control media with
332 excess glucose and found that although oxidative stress was slightly improved when
333 *PfCM* was supplemented with excess glucose as compared to *PfCM* without excess
334 glucose, there was still a significant increase in intracellular ROS **(Supplemental Figure**
335 **4A)**. As recent work has demonstrated that free mitochondrial DNA can stimulate TLR9
336 responses in RBCs and induce morphological changes (e.g., echinocytosis and
337 increased rigidity)¹⁰, we wanted to know whether our *PfCM* also had elevated
338 mitochondrial DNA and whether this coincided with the increase in intracellular ROS.

339 Indeed, when we performed quantitative PCR for CPG-containing mitochondrial DNA in
340 the *PfCM* exposed RBCs, we corroborated recently published findings by Lam *et al.* and
341 we did see an association between the conditions with elevated mitochondrial DNA and
342 elevated intracellular ROS¹⁰.

343

344 **QCG supplementation lessens *PfCM*-induced oxidative stress in RBCs**

345 We next aimed to determine whether QCG supplementation also conferred protection to
346 RBCs exposed to *PfCM*. Indeed, RBCs pretreated with QCG amino acids were found to
347 have a significant reduction in intracellular ROS following *PfCM* incubation (mean fold
348 change of 1.72 for 0 μ M QCG vs. 1.15 for 1000 μ M QCG, $p = 0.027$) (**Figure 4A**).

349 Morphologically, we observed RBCs pretreated with QCG had overall improved
350 morphology scores after *PfCM* stress (mean score of 130 for 0 μ M QCG vs. 122 for
351 1000 μ M QCG, $p = 0.040$) (**Figure 4B**). Therefore, we found that QCG supplementation
352 confers protection to *PfCM*-induced oxidative stress in RBCs and that decreased
353 intracellular ROS levels coincided with improved RBC morphology. We did not however
354 find that QCG supplementation had any effect on lessening the amount of mtDNA,
355 suggesting that QCG supplementation does not work through depleting the amount of
356 mtDNA stressor in the media (**Supplemental Figure 4B**).

357

358 **QCG supplementation induces intracellular RBC glutathione synthesis**

359 We hypothesized that QCG protection occurs via intracellular GSH metabolic pathways
360 given that each amino acid is a known precursor for *de novo* GSH synthesis (**Figure**
361 **5A**). We found increased levels of total glutathione in QCG-supplemented RBCs
362 (**Figures 5B-D, Supplementary Figures 5A-C**). This activity was evident from QCG
363 supplementation, with or without induced oxidative stress. We also observed an
364 increased level of oxidized glutathione (GSSG) in QCG supplemented RBCs after

365 exposure to either *PfCM* (1525 mean peak area intensity for 0 μM QCG vs 6725 for
366 1000 μM QCG, $p = 0.009$) (**Figure 5C**) or H_2O_2 (111,650 mean peak area intensity for 0
367 μM QCG vs 211,245 for 1000 μM QCG, $p = 0.103$) (**Supplemental Figure 5B**)
368 compared to RBCs without QCG supplementation or exposure to oxidative stress. These
369 results indicate that QCG supplemented RBCs have increased intracellular glutathione
370 biosynthesis.

371

372 **Supplementation with QCG promotes RBC intrinsic antioxidant properties**

373 Given the aforementioned findings, it remained unclear whether QCG-mediated
374 protection was a generalized RBC response or if QCG protection occurred specifically
375 under oxidative stress exposure. To determine this, we analyzed the kinetic response of
376 QCG supplemented RBCs to oxidative stress. RBCs pre-exposed to QCG showed lower
377 levels of intracellular ROS within 2.5 min of H_2O_2 -induced oxidative stress while RBCs
378 pre-exposed to either PBS or Gln had higher levels of ROS that developed quicker
379 within the cells (**Figure 6A**). Cellular response to oxidative stress among all
380 preincubation conditions appeared to be heterogenous across cells (**Figures 6B-D**) and
381 interestingly, we observed punctate-like areas of increased fluorescence in each
382 preincubation condition with or without H_2O_2 -induced oxidative stress, suggesting
383 internal organization of intracellular ROS with morphology consistent with that of Heinz-
384 Ehrlich bodies. This phenomenon was observed in both H_2O_2 and *PfCM*-stressed RBCs
385 (**Figure 6E**). Together, these data indicate QCG preincubation intrinsically prepares
386 RBCs to counter oxidative stress prior to any oxidative stress exposure rather than
387 mounting an antioxidant response directly following oxidative stress.

388

389

390 **Discussion**

391 In this study, we investigated the metabolic role of amino acid supplementation on
392 oxidatively stressed RBCs with an overall goal of alleviating RBC oxidative burden. We
393 first explored Gln supplementation on RBCs stressed by H₂O₂ and observed that while
394 Gln supplementation alone was not sufficient to reduce oxidative stress levels within
395 RBCs, Gln supplementation promoted RBC hydration (**Figure 1**). In contrast, we
396 identified a significant decrease in intracellular ROS in RBCs that had been
397 supplemented with QCG amino acids (**Figure 2**). These data suggest that observed
398 ROS protection is conferred through RBC GSH biosynthesis pathway, as total
399 glutathione was increased in RBCs supplemented with QCG (**Figure 5**) and this
400 protection from intracellular ROS development was found to be rapid (2.5 min) upon
401 induction of oxidative stress (**Figure 6**). Interestingly, single amino acid supplementation
402 did not reduce intracellular ROS, an effect we only saw with simultaneous
403 supplementation with QCG (**Supplemental Figure 2**). Post-exposure of QCG did not
404 have a comparable protection to RBCs that were oxidatively stressed first (data not
405 shown), suggesting that utilization of QCG is done to equip RBCs to defend themselves
406 against any oxidative stress they may incur in the future. Here, we also report for the first
407 time to our knowledge that conditioned media from *P. falciparum* culture increases
408 intracellular ROS in uninfected, catalase-depleted RBCs (**Figure 3**), and is a likely
409 contributor to malaria bystander effect. Additionally, we found that QCG supplementation
410 does indeed confer protection in the form of reduced intracellular ROS and improved
411 echinocyte morphology to *PfCM* stressed RBCs (**Figure 4**) despite the inhibition of
412 catalase in these RBCs, highlighting a therapeutic prospect for malarial anemia.

413

414 Recently *PfCM* was shown to increase oxidative stress in erythroid precursor cells⁹ and
415 alter membrane structure and binding in uninfected mature RBCs¹⁰. However, it was
416 unclear if *PfCM* also perturbed the oxidative status of uninfected mature RBCs. We

417 confirmed one mode of action that *PfCM* has on mature, catalase-depleted RBCs is
418 through oxidative stress as measured by the induction of intracellular ROS. In general,
419 elevated ROS reduces RBC survivability *in vivo*⁴⁹, suggesting this could be an additional
420 contributor to pathogenesis of bystander effect in malaria.

421

422 Gln is implicated in both sickle cell anemia and malarial anemia, highlighting a possible
423 role for metabolic intervention in anemic conditions. Lower plasma Gln levels are
424 associated with pediatric malarial anemia³⁰ while oral Gln supplementation is an
425 approved treatment for sickle cell anemia, although cellular mechanisms of this therapy
426 are still under investigation. Here, we show that Gln supplementation improves RBC
427 hydration status, a potential mechanistic role that warrants more investigation
428 specifically in sickle RBCs. It is long appreciated that RBCs respond to exogenous
429 metabolites and that the lack of necessary exogenous metabolites negatively impacts
430 RBC lifespan^{50,51}. Prior to this study, it was unknown how pre-exposure to exogenous
431 amino acids impacted RBCs in the context of oxidative stress and malaria bystander
432 effect. Our study design of amino acid supplementation was focused on recapitulating
433 the plasma environment if key metabolites were supplemented in advance of infection or
434 oxidative stress. We found that RBCs supplemented with QCG amino acids are
435 equipped to counter oxidative stress from both H₂O₂ and *PfCM*. We showed that this
436 benefit was intrinsic to RBCs and that ROS development was mitigated within minutes in
437 the cell. As intracellular GSH synthesis occurs in the order of hours within RBCs^{17,52}, this
438 suggests that GSH stores increase in response to QCG pre-incubation, and are not a
439 combative cellular response to oxidative stress. Glutamine is an important precursor to
440 arginine *in vivo* via citric acid cycle and mitochondrial pathways and supplementation
441 with arginine is reported to be beneficial in both malaria²⁸ and sickle cell anemia²⁹. Within
442 the context of RBCs as reported in this study, arginine supplementation did not confer

443 oxidative protection intracellularly, suggesting that the beneficial role of arginine, and
444 therefore glutamine as an arginine precursor, requires pathways that are active in
445 nucleated cells rather than in RBCs. Collectively, our results highlight a beneficial role for
446 exogenous QCG to RBCs prior to oxidative stress. These findings may suggest a
447 prophylactic or therapeutic role of amino acid supplementation in oxidative anemias,
448 including in malaria.

449

450 Our study had limitations. First, these experiments were performed *in vitro* with only
451 RBCs present. However, in an *in vivo* context, RBC exogenous amino acid availability
452 and utilization would be complicated by other cells present which also can utilize these
453 substrates. Secondly, we induced oxidative stress in RBCs under the presence of
454 sodium azide, a known inhibitor of the catalase enzyme, to model stressed uninfected
455 RBCs from *P. falciparum* culture and malaria infected patients that have been shown to
456 have significantly reduced catalase levels^{16,53}, it is important to acknowledge that
457 complete ablation using sodium azide is a non-physiological model and is more severe
458 than what is experienced by RBCs under physiological conditions. Third, we are unable
459 to comment on the exogenous bioavailability and utilization of QCG by RBCs in an *in*
460 *vivo* context, as these studies focused on cellular, *in vitro* effects of QCG
461 supplementation. More studies would need to be performed in *in vivo* systems. In terms
462 of our measurement of ROS, we performed one assay, DCFDA, which provides a
463 general measure of intracellular ROS, but further studies using additional probes to
464 better confirm and define the type(s) of ROS in the cell would be valuable. It is also
465 challenging to determine the extent of clinical significance through measuring
466 deformability. While effects may be small, any amount of reduced deformability reflects
467 rheological deficiencies that could be tied to increased blood viscosity and propensity for
468 hemolysis. The fact that QCG supplementation shows a significant improvement after an

469 acute insult with H₂O₂ coupled with catalase inhibition may translate to clinical
470 improvements in contexts in which insults are prolonged. For example, in severe
471 malarial anemia, prolonged exposure to oxidative stress could reduce RBCs'
472 endogenous antioxidant capacity (e.g., intracellular glutathione stores) and exogenous
473 amino acids could serve as essential building blocks for build back up those internal
474 stores. A strength but also a limitation of our study is that we use different human
475 participants in the various experiments shown. On one hand, this shows the broad
476 applicability of these findings to different humans, but on the other hand, we do not have
477 one set of human participants that we have analyzed side-by-side in all experiments. As
478 such, there is a certain amount of human-to-human variability that we have as part of
479 this study. Finally, while we find an association between intracellular ROS and altered
480 RBC morphology as have others⁵⁴, we cannot definitively conclude that this is a
481 causative relationship. Future work must be done to fully decipher the mechanistic
482 processes underlying RBC morphology change in the context of exogenous stressors.

483

484 **Acknowledgments**

485 This research was supported in part by the National Institutes of Health (NIH) National
486 Heart, Lung and Blood Institute (K01HL143112, RJC). RJC was also supported by the
487 Programs to Increase Diversity Among Individuals Engaged in Health-Related Research
488 - Functional and Translational Genomics of Blood Disorders Program (PRIDE-FTG) at
489 Augusta University (R25HL106365). HCB was supported by NIH National Institute of
490 General Medical Sciences (T32GM127261). CES was supported by NIH National
491 Institute of General Medical Sciences (T32 GM149818). This research was also
492 supported by awards from Wake Forest University Center for Molecular Signaling and
493 the Wake Forest University School of Medicine Center for Redox Biology and Medicine.
494 The authors also acknowledge the Wake Forest Baptist Comprehensive Cancer Center

495 Proteomics and Metabolomics Shared Resource supported by the National Cancer
496 Institute's Cancer Center Support Grant award number P30CA012197 and the
497 Microscopic Imaging Core supported by the Wake Forest Department of Biology. Drs.
498 Betty Pace and Mohandas Narla are acknowledged for their mentorship and feedback,
499 and Jordan Buzzett, Kevin Coffey and Ryan Marie Kelly are acknowledged for their
500 laboratory assistance. Graphical images were created with BioRender.com.

501

502

503 **Author Contributions**

504 R.J.C. and H.C.B. designed and conceptualized the project; H.C.B. performed and
505 analyzed the results of the experiments, designed the figures, and wrote the initial
506 manuscript. E.A. performed and analyzed ektacytometry experiments. C.E.S. performed
507 flow cytometry experiments. D.S.N. performed parasite culture and conditioned media
508 generation. J.F.W. contributed technical expertise for flow cytometry experiments.
509 A.O.C. performed mass spectrometry experiments. C.M.F. supervised mass
510 spectrometry and contributed redox biology expertise. G.S.M. assisted with microscopy
511 experiments and contributed technical expertise for fluorescent and scanning electron
512 microscopy imaging. D.B.K-S. supervised ektacytometry, contributed red cell biophysics
513 expertise, and contributed to the overall experimental design. R.J.C. supervised the
514 experiments, data analysis, and revising of the manuscript. All authors contributed to
515 and endorsed the final version of the manuscript.

516

517 **Disclosure of Conflicts of Interest**

518 The authors do not have any conflicts of interest to disclose.

519

520 **Figure Legends**

521

522 **Figure 1: Glutamine pre-treatment benefitted oxidatively stressed RBCs through**
523 **osmotic protection**

524 (A) Fold change of intracellular ROS detected by DCFDA staining and flow cytometry in
525 RBCs. (B) Representative ektacytometry curve as cells pass through osmotic gradient at
526 a constant shear stress of 16 Pa. (C) Maximum deformability index (DI_{max}) values and
527 (D) RBC hydration graphed as O_{hyper} ; n=3. Mean \pm standard error of the mean denoted
528 by error bars. One-way paired t-test; ns = not significant, * $p < 0.05$

529

530 **Figure 2: QCG preincubation reduces oxidative impact of H₂O₂ induced stress**

531 (A) Fold change of intracellular ROS detected by DCFDA staining and flow cytometry in
532 RBCs; n=6 (B) Representative ektacytometry curve as cells pass through osmotic
533 gradient at a constant shear stress of 16 Pa. (C) Maximum deformability and (D)
534 hydration level of RBCs from ektacytometry curves; n=3. Mean \pm standard error of the
535 mean denoted by error bars. One-way paired t-test; ns = not significant, * $p < 0.05$, ** $p <$
536 0.005 , *** $p < 0.0005$.

537

538 **Figure 3: PfCM increases RBC echinocytosis and intracellular ROS**

539 RBCs incubated in control media or PfCM overnight were imaged with Scanning
540 Electron Microscopy (AMRAY 1810, 2000X total magnification) and assessed based on
541 (A) morphology scores and (B) percentage echinocytes (n=7). RBCs incubated in
542 control media or PfCM overnight were washed after incubations and stained with
543 DCFDA to quantify intracellular ROS with flow cytometry. Representative flow cytometry
544 histogram shown in (C) and bar graph of ROS fold change compared to control in (D);

545 n=4. Mean \pm standard error of the mean denoted by error bars. One-way paired t-test; *p
546 < 0.05, ** p < 0.005, *** p<0.0005.

547

548 **Figure 4: QCG supplementation protects RBCs from PfCM induced oxidative**
549 **stress**

550 (A) Fold change of intracellular ROS detected by DCFDA staining and flow cytometry in
551 RBCs, n=3. (B) RBC morphology score assessed from scanning electron microscopy
552 images, n=5. Mean \pm standard error of the mean denoted by error bars. One-way paired
553 t-test; ns = not significant, *p < 0.05

554

555 **Figure 5: Glutathione metabolic changes within RBCs supplemented with QCG**

556 **followed by PfCM stress** (A) Schematic of metabolic processes known to occur within
557 RBCs from QCG amino acids. Peak area intensity of (B) reduced glutathione (GSH), (C)
558 oxidized glutathione (GSSG), and (D) total glutathione as measured by LC-MS/MS, n=3.
559 One-way paired t-test; ns = not significant, *p < 0.05, ** p < 0.005.

560

561 **Figure 6: QCG supplementation rapidly protects RBCs from intracellular ROS**
562 **formation during oxidative stress**

563 RBCs pretreated with either PBS, Gln (Q), or QCG were labeled with DCFDA and
564 placed in a glass bottom petri dish per sample condition and allowed to settle for 45
565 seconds before given a bolus (red arrow, A) of PBS (grey line, B-D) or 50 μ M H₂O₂ (red
566 line, B-D). Stationary cells (total 8 cells per condition) were quantified (A) and imaged
567 (B-D) per condition at each 15 second time point for five minutes. Images were taken
568 with Leica Thunder at 63X oil immersion (A-D). Representative images of DCFDA

569 labeled RBCs stressed with 50 μM H_2O_2 (left) or *Pf*CM (right) (E). Images taken with
570 Echo Revolve Fluorescent Microscope at 100X oil immersion (E).

571

572

573 **References**

- 574 1. Global Malaria Programme. World malaria report 2022.
- 575 2. Lamikanra AA, Brown D, Potocnik A, et al. Malarial anemia: of mice and men.
576 *Blood*. 2007;110(1):18–28.
- 577 3. Jakeman GN, Saul A, Hogarth WL, Collins WE. Anaemia of acute malaria
578 infections in non-immune patients primarily results from destruction of
579 uninfected erythrocytes. *Parasitology*. 1999;119(2):127–133.
- 580 4. Dondorp AM, Nyanoti M, Kager PA, et al. The role of reduced red cell
581 deformability in the pathogenesis of severe falciparum malaria and its
582 restoration by blood transfusion. *Transactions of the Royal Society of Tropical*
583 *Medicine and Hygiene*. 2002;96(3):282–286.
- 584 5. Barber BE, Russell B, Grigg MJ, et al. Reduced red blood cell deformability in
585 *Plasmodium knowlesi* malaria. 2018;
- 586 6. Dasari P, Fries A, Heber SD, et al. Malarial anemia: digestive vacuole of
587 *Plasmodium falciparum* mediates complement deposition on bystander cells
588 to provoke hemophagocytosis. *Med Microbiol Immunol*. 2014;203(6):383–
589 393.
- 590 7. Fernandez-Arias C, Rivera-Correa J, Gallego-Delgado J, et al. Anti-Self
591 Phosphatidylserine Antibodies Recognize Uninfected Erythrocytes Promoting
592 Malarial Anemia. *Cell Host & Microbe*. 2016;19(2):194–203.

- 593 8. Fonseca LL, Alezi HS, Moreno A, et al. Quantifying the removal of red blood
594 cells in *Macaca mulatta* during a *Plasmodium coatneyi* infection. *Malaria*
595 *Journal*. 2016;15:410.
- 596 9. Neveu G, Richard C, Dupuy F, et al. *Plasmodium falciparum* sexual parasites
597 develop in human erythroblasts and affect erythropoiesis. *Blood*.
598 2020;136(12):1381–1393.
- 599 10. Lam LKM, Murphy S, Kokkinaki D, et al. DNA binding to TLR9 expressed by
600 red blood cells promotes innate immune activation and anemia. *Sci. Transl.*
601 *Med*. 2021;13(616):eabj1008.
- 602 11. Jezewski AJ, Lin Y-H, Reisz JA, et al. Targeting Host Glycolysis as a Strategy
603 for Antimalarial Development. *Front. Cell. Infect. Microbiol*. 2021;11:730413.
- 604 12. Suzuki T, Agar NS, Suzuki M. Red blood cell metabolism in experimental
605 animals: pentose phosphate pathway, antioxidant enzymes and glutathione.
606 *Jikken Dobutsu*. 1985;34(4):353–366.
- 607 13. Low FM, Hampton MB, Winterbourn CC. Peroxiredoxin 2 and Peroxide
608 Metabolism in the Erythrocyte. *Antioxidants & Redox Signaling*.
609 2008;10(9):1621–1630.
- 610 14. Percário S, Moreira D, Gomes B, et al. Oxidative Stress in Malaria. *IJMS*.
611 2012;13(12):16346–16372.
- 612 15. Antwi-Boasiako C, Dankwah G, Aryee R, et al. Oxidative Profile of Patients
613 with Sickle Cell Disease. *Medical Sciences*. 2019;7(2):17.

- 614 16. Areekul S, Boonme Y. Superoxide dismutase and catalase activities in red
615 cells of patients with Plasmodium falciparum. *J Med Assoc Thai*.
616 1987;70(3):127–131.
- 617 17. Raftos JE, Whillier S, Kuchel PW. Glutathione Synthesis and Turnover in the
618 Human Erythrocyte. *Journal of Biological Chemistry*. 2010;285(31):23557–
619 23567.
- 620 18. Cordy RJ, Patrapuvich R, Lili LN, et al. Distinct amino acid and lipid
621 perturbations characterize acute versus chronic malaria. *JCI Insight*.
622 2019;4(9):.
- 623 19. Beri D, Ramdani G, Balan B, et al. Insights into physiological roles of unique
624 metabolites released from Plasmodium-infected RBCs and their potential as
625 clinical biomarkers for malaria. *Scientific Reports*. 2019;9(1):2875.
- 626 20. Leopold SJ, Apinan S, Ghose A, et al. Amino acid derangements in adults
627 with severe falciparum malaria. *Scientific Reports*. 2019;9(1):.
- 628 21. Leopold SJ, Ghose A, Allman EL, et al. Identifying the Components of
629 Acidosis in Patients with Severe Plasmodium falciparum Malaria Using
630 Metabolomics. *Journal of Infectious Diseases*. 2019;219(11):1766–1776.
- 631 22. Lopansri BK, Anstey NM, Weinberg JB, et al. Low plasma arginine
632 concentrations in children with cerebral malaria and decreased nitric oxide
633 production. *The Lancet*. 2003;361(9358):676–678.
- 634 23. Lakshmanan V, Rhee KY, Wang W, et al. Metabolomic analysis of patient
635 plasma yields evidence of plant-like α -linolenic acid metabolism in
636 Plasmodium falciparum. *J. Infect. Dis*. 2012;206(2):238–248.

- 637 24. Colvin HN, Cordy RJ. Insights into malaria pathogenesis gained from host
638 metabolomics. *PLoS Pathog.* 2020;16(11):e1008930.
- 639 25. Gupta S, Seydel K, Miranda-Roman MA, et al. Extensive alterations of blood
640 metabolites in pediatric cerebral malaria. *PLoS ONE.* 2017;12(4):.
- 641 26. Niihara Y, Miller ST, Kanter J, et al. A Phase 3 Trial of L-Glutamine in Sickle
642 Cell Disease. *New England Journal of Medicine.* 2018;379(3):226–235.
- 643 27. Kanne CK, Reddy V, Sheehan VA. Rheological Effects of L-Glutamine in
644 Patients with Sickle Cell Disease. *Blood.* 2019;134(Supplement_1):3567–
645 3567.
- 646 28. Ong PK, Moreira AS, Daniel-Ribeiro CT, Frangos JA, Carvalho LJM.
647 Reversal of cerebrovascular constriction in experimental cerebral malaria by
648 L-arginine. *Sci Rep.* 2018;8(1):15957.
- 649 29. Little JA, Hauser KP, Martyr SE, et al. Hematologic, biochemical, and
650 cardiopulmonary effects of L - arginine supplementation or
651 phosphodiesterase 5 inhibition in patients with sickle cell disease who are on
652 hydroxyurea therapy. *European J of Haematology.* 2009;82(4):315–321.
- 653 30. Kempaiah P, Dokladny K, Karim Z, et al. Reduced Hsp70 and Glutamine in
654 Pediatric Severe Malaria Anemia: Role of hemozoin in Suppressing Hsp70
655 and NF-κB Activation. *Molecular Medicine.* 2016;22(1):570–584.
- 656 31. Low FM, Hampton MB, Peskin AV, Winterbourn CC. Peroxiredoxin 2
657 functions as a noncatalytic scavenger of low-level hydrogen peroxide in the
658 erythrocyte. *Blood.* 2007;109(6):2611–2617.

- 659 32. Nuchsongsin F, Chotivanich K, Charunwatthana P, et al. Effects of malaria
660 heme products on red blood cell deformability. *American Journal of Tropical*
661 *Medicine and Hygiene*. 2007;77(4):617–622.
- 662 33. Snyder LM, Fortier NL, Trainor J, et al. Effect of hydrogen peroxide exposure
663 on normal human erythrocyte deformability, morphology, surface
664 characteristics, and spectrin-hemoglobin cross-linking. *J. Clin. Invest.*
665 1985;76(5):1971–1977.
- 666 34. Srivastava K, Singh S, Singh P, Puri SK. In vitro cultivation of Plasmodium
667 falciparum: Studies with modified medium supplemented with ALBUMAX II
668 and various animal sera. *Experimental Parasitology*. 2007;116(2):171–174.
- 669 35. Mbagwu S, Walch M, Filgueira L, Mantel P-Y. Production and
670 Characterization of Extracellular Vesicles in Malaria. *Extracellular Vesicles*.
671 2017;1660:377–388.
- 672 36. Schindelin J, Arganda-Carreras I, Frise E, et al. Fiji: an open-source platform
673 for biological-image analysis. *Nat Methods*. 2012;9(7):676–682.
- 674 37. Colvin HN, Marrs, Glen, Cordy, Regina Joice. Osmolality-controlled fixation
675 and simple preparation of human red blood cells for scanning electron
676 microscopy. *protocols.io*. 2022;
- 677 38. Geekiyanage NM, Balanant MA, Sauret E, et al. A coarse-grained red blood
678 cell membrane model to study stomatocyte-discocyte-echinocyte
679 morphologies. *PLoS ONE*. 2019;14(4):e0215447.

- 680 39. Immerman KL, Melaragno AJ, Quellet RP, Weinstein R, Valeri CR.
681 Morphology of glutaraldehyde-fixed preserved red blood cells and 24-hr post-
682 transfusion survival. *Cryobiology*. 1983;20(1):30–35.
- 683 40. Bessis M, Weed RI. The Structure of Normal and Pathologic Erythrocytes.
684 *Advances in Biological and Medical Physics*. 1973;14:35–91.
- 685 41. Atkins HM, Bharadwaj MS, O'Brien Cox A, et al. Endometrium and
686 endometriosis tissue mitochondrial energy metabolism in a nonhuman
687 primate model. *Reprod Biol Endocrinol*. 2019;17(1):70.
- 688 42. Sun X, Berger RS, Heinrich P, et al. Optimized Protocol for the In Situ
689 Derivatization of Glutathione with N-Ethylmaleimide in Cultured Cells and the
690 Simultaneous Determination of Glutathione/Glutathione Disulfide Ratio by
691 HPLC-UV-QTOF-MS. *Metabolites*. 2020;10(7):292.
- 692 43. Kuypers FA, Scott MD, Schott MA, Lubin B, Chiu DT. Use of ektacytometry to
693 determine red cell susceptibility to oxidative stress. *J Lab Clin Med*.
694 1990;116(4):535–545.
- 695 44. Clark M, Mohandas N, Shohet S. Osmotic gradient ektacytometry:
696 comprehensive characterization of red cell volume and surface maintenance.
697 *Blood*. 1983;61(5):899–910.
- 698 45. Ellory JC, Preston RL, Osotimehin B, Young JD. Transport of amino acids for
699 glutathione biosynthesis in human and dog red cells. *Biomed Biochim Acta*.
700 1983;42(11–12):S48-52.
- 701 46. Newsholme P, Lima MMR, Procopio J, et al. Glutamine and glutamate as vital
702 metabolites. *Braz J Med Biol Res*. 2003;36(2):153–163.

- 703 47. Ruggeri F, Marcott C, Dinarelli S, et al. Identification of Oxidative Stress in
704 Red Blood Cells with Nanoscale Chemical Resolution by Infrared
705 Nanospectroscopy. *IJMS*. 2018;19(9):2582.
- 706 48. Jensen MD, Conley M, Helstowski LD. Culture of Plasmodium falciparum: the
707 role of pH, glucose, and lactate. *J Parasitol*. 1983;69(6):1060–1067.
- 708 49. Kumar D, Rizvi SI. Markers of Oxidative Stress in Senescent Erythrocytes
709 Obtained from Young and Old Age Rats. *Rejuvenation Research*.
710 2014;17(5):446–452.
- 711 50. Tunnicliff G. Amino acid transport by human erythrocyte membranes.
712 *Comparative Biochemistry and Physiology Part A: Physiology*.
713 1994;108(4):471–478.
- 714 51. Zolla L, D'Alessandro A. Classic and alternative red blood cell storage
715 strategies: seven years of “-omics” investigations. *Blood Transfusion*. 2015;
- 716 52. Whillier S, Garcia B, Chapman BE, Kuchel PW, Raftos JE. Glutamine and α -
717 ketoglutarate as glutamate sources for glutathione synthesis in human
718 erythrocytes: Glutamate sources for glutathione synthesis. *FEBS Journal*.
719 2011;278(17):3152–3163.
- 720 53. Areekul S, Churdchu K, Thanomsak W, et al. Superoxide dismutase and
721 catalase activities of cultured erythrocytes infected with Plasmodium
722 falciparum. *Southeast Asian J Trop Med Public Health*. 1988;19(4):601–607.
- 723 54. Hale JP, Winlove CP, Petrov PG. Effect of hydroperoxides on red blood cell
724 membrane mechanical properties. *Biophys J*. 2011;101(8):1921–1929.
- 725

Figure 1_31OCT2023

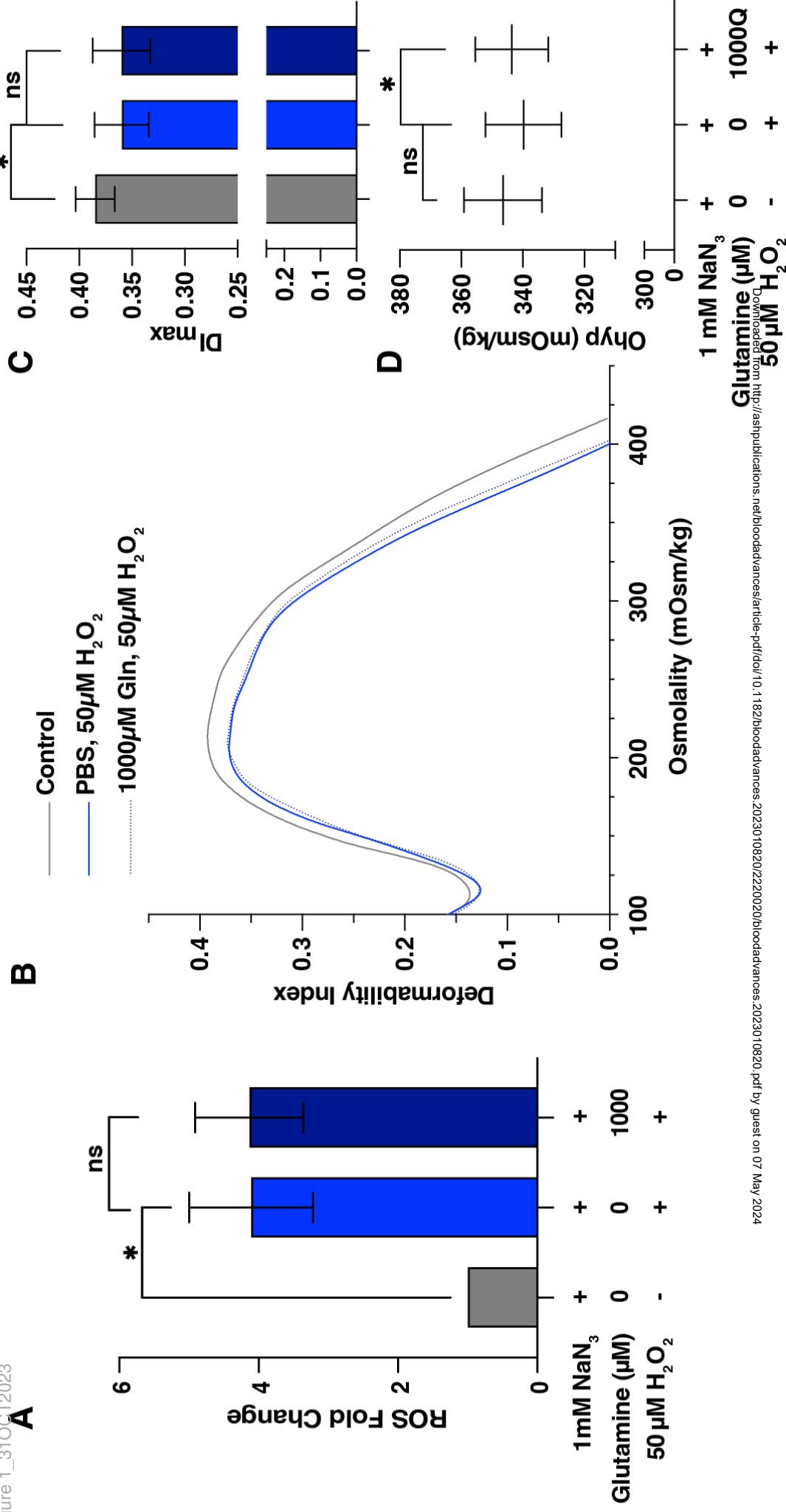
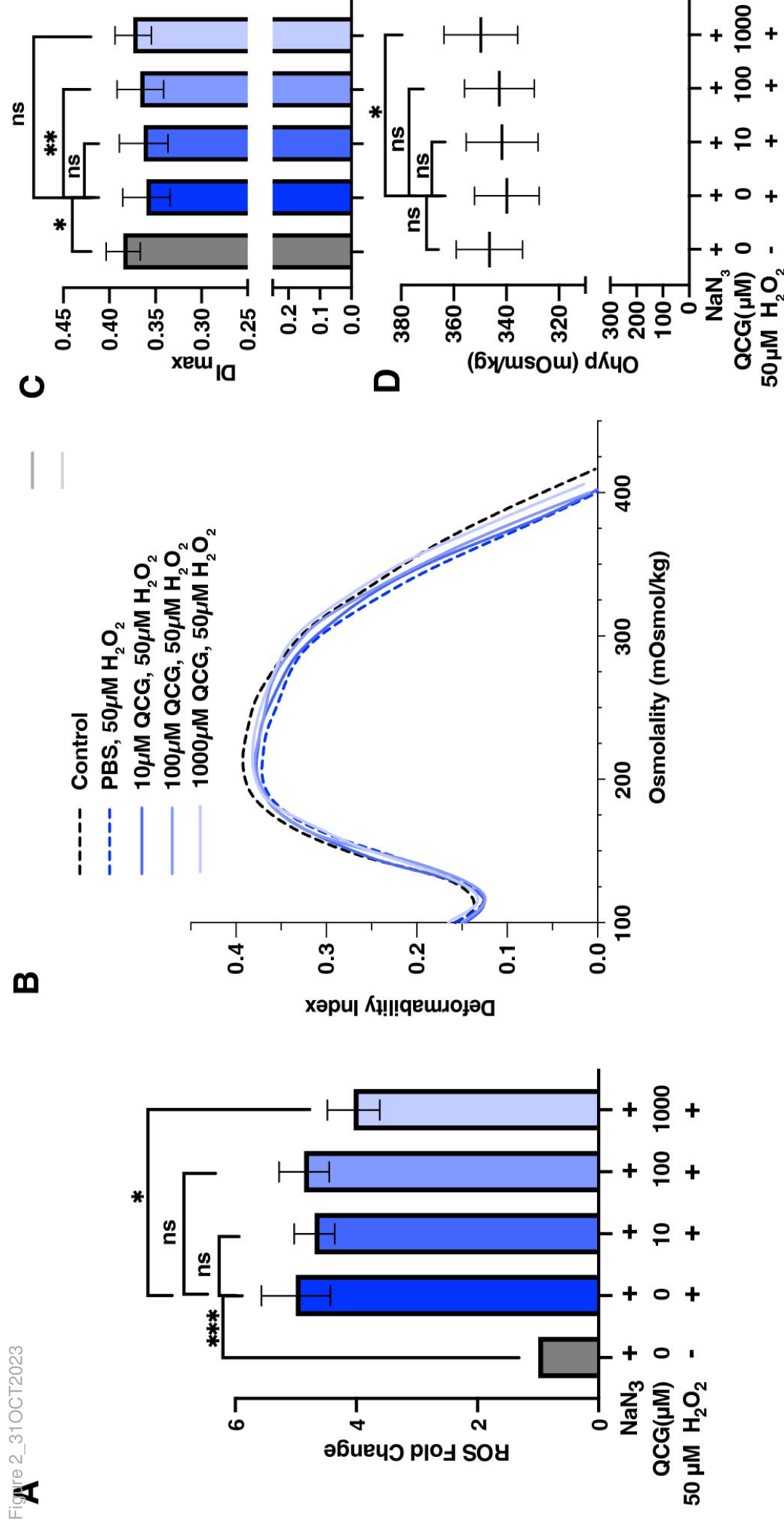


Figure 2_31OCT2023



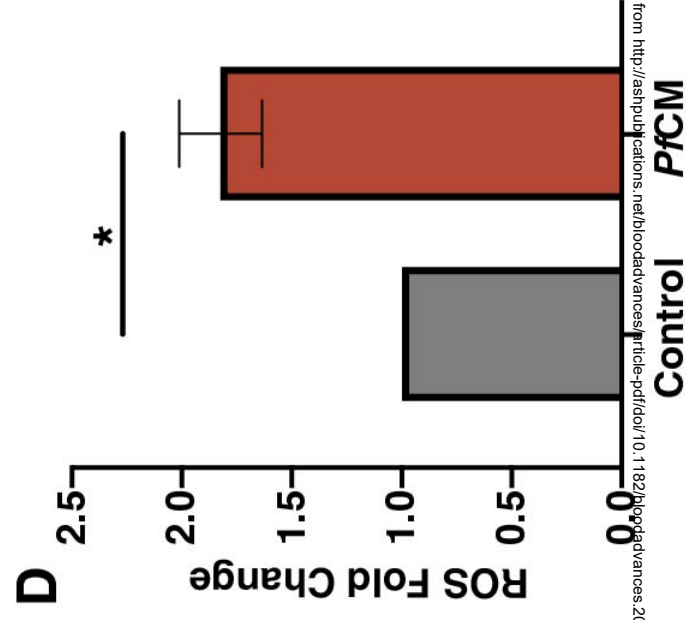
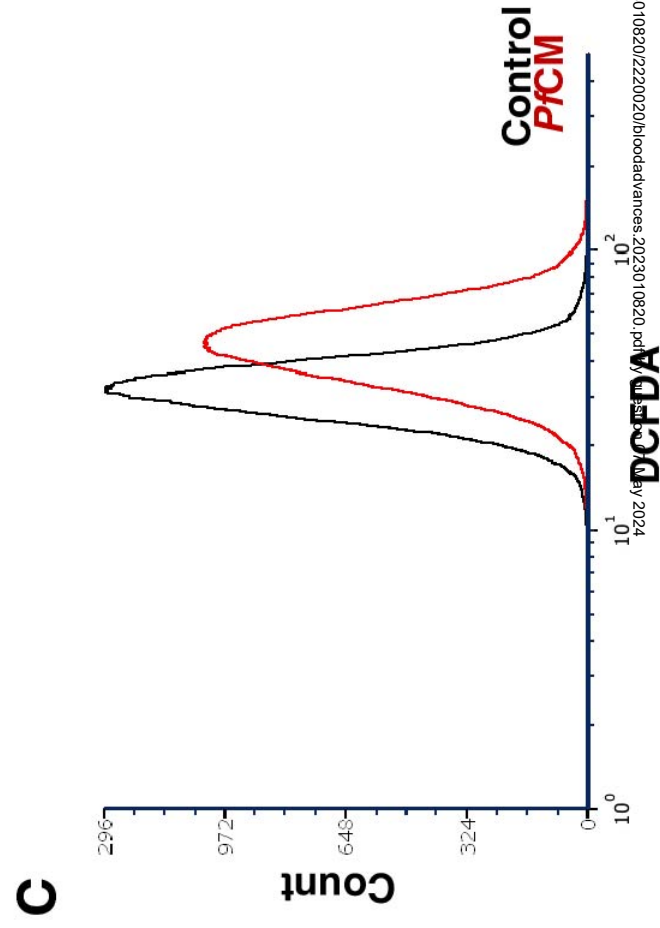
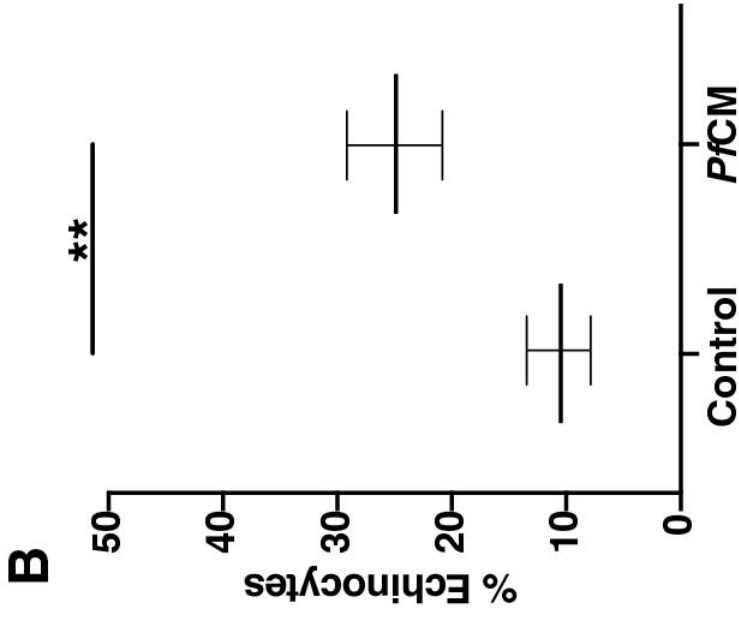
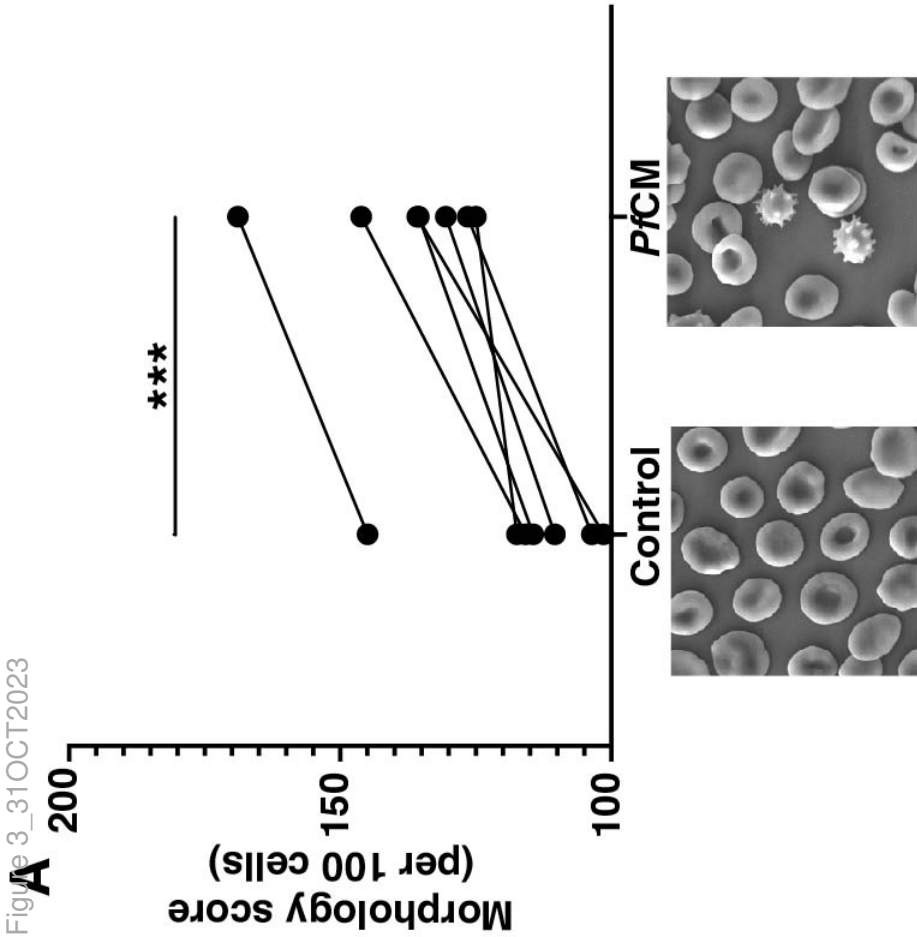
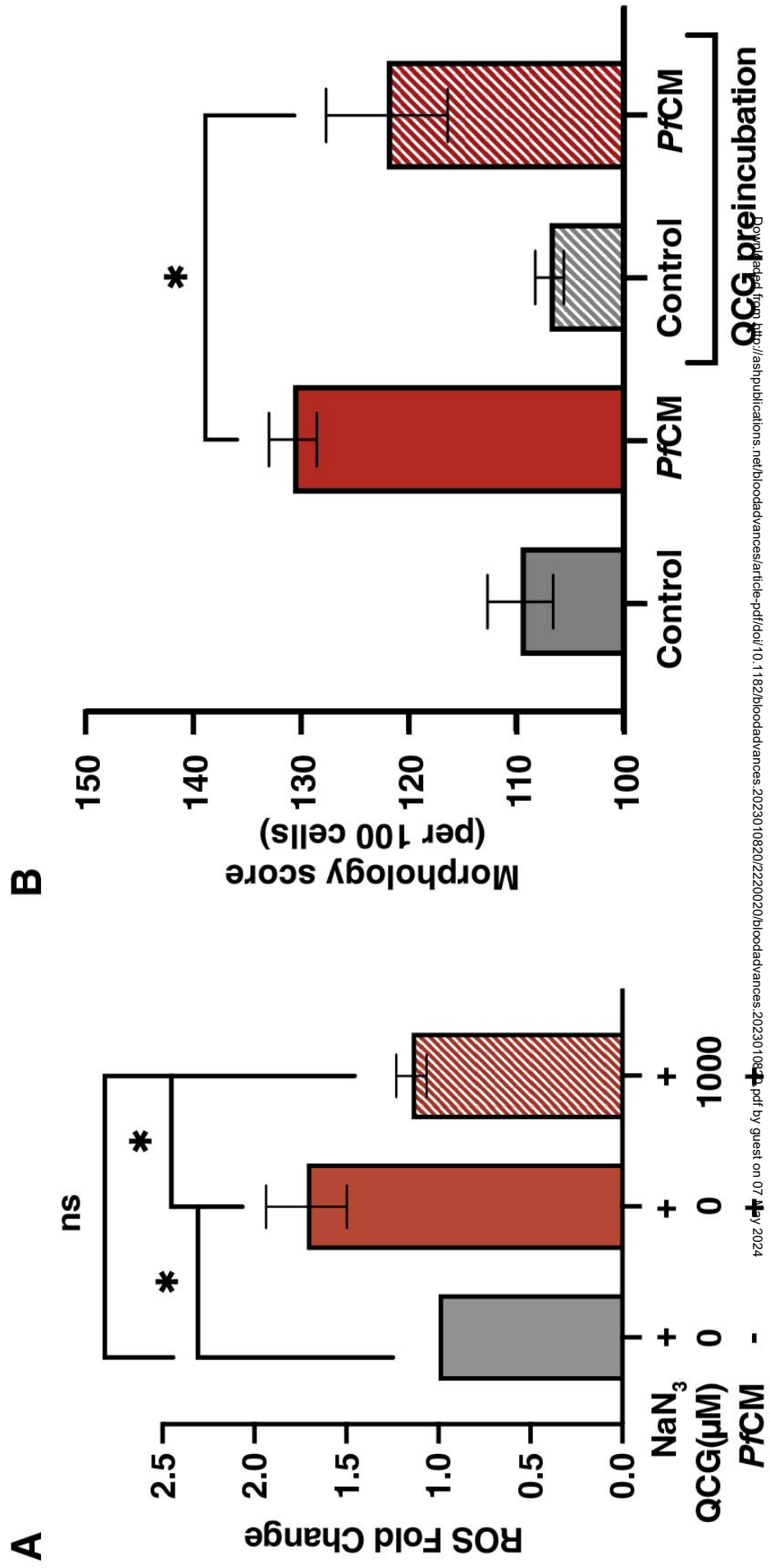


Figure 4_31OCT2023



A Figure 5

